Surface Science 432 (1999) 115–124
surface science
www.elsevier.nl/locate/susc

LEEM investigation of the faceting of the Pt covered W(111) surface

K. Pelhos [a], J.B. Hannon [b], G.L. Kellogg [b], T.E. Madey [a,*]

[a] *Department of Physics and Astronomy and Laboratory for Surface Modification, Rutgers, The State University of New Jersey, 136 Frelinghuysen Road, Piscataway, NJ 08854-8019, USA*
[b] *Sandia National Laboratories, Albuquerque, NM, USA*

Received 15 January 1999; accepted for publication 5 April 1999

Abstract

A low energy electron microscope has been used to investigate the faceting of W(111) as induced by Pt. The atomically rough W(111) surface, when fully covered with a monolayer film of Pt and annealed to temperatures higher than ~750 K, experiences a significant morphological restructuring: the initially planar surface undergoes a faceting transition and forms three-sided pyramids with {211} faces. The experiments demonstrate the capability of low energy electron microscopy for imaging both the fully and the partially faceted surface. In addition, we have observed the formation of the facets in real time, when Pt is dosed onto the heated surface. We find that the transition from planar surface, to partially faceted surface, and to fully faceted surface proceeds through the nucleation and growth of spatially separated faceted regions. © 1999 Elsevier Science B.V. All rights reserved.

Keywords: Faceting; Growth; Low-energy electron microscopy (LEEM); Nucleation; Platinum; Surface diffusion; Tungsten

1. Introduction

Model bimetallic catalysts consisting of thin metal films deposited onto planar single crystal metal surfaces are of great interest to surface scientists because of their interesting physical and chemical characteristics. We have focused recently on studying a special class of bimetallic systems: films up to a few atomic layers thick on the atomically rough (111) surface of bcc metals, such as W and Mo. A special emphasis is placed on the morphological stability of these systems, as certain overlayer films are found to induce a large scale restructuring of the substrate under certain conditions, forming nanoscale facets. Specifically, W(111) and Mo(111) surfaces are found to be morphologically unstable when covered by ultrathin films of Pt, Pd, Au, Rh or Ir; pyramidal facets are formed when the film covered surface is annealed to temperatures above ~750 K [1–3]. The sides of the pyramids have mainly {211} orientations as evidenced by both low energy electron diffraction (LEED) and scanning tunneling microscopy (STM). STM also shows that depending on annealing temperatures and times these facets can grow as large as ~100 Å (in the case of Pd) up to a maximum size of ~1500 Å (in the case of Pt).

There are scientific issues, however, that are yet to be addressed in connection with metal overlayer induced faceting of W and Mo(111). These include the nature of facet nucleation, coexistence of faceted and planar surfaces, facet growth (with annea-

* Corresponding author. Fax: +1 732 445 4991.
E-mail address: madey@physics.rutgers.edu (T.E. Madey)

0039-6028/99/$ – see front matter
PII: S0039-6028(99)00543-9

ling time), and a high temperature *reversible* transition from faceted to planar surface [4]. In the present work we use a low energy electron microscope [5] to provide new insights into the Pt induced faceting of W(111). Our main objective is to conduct real-time observations of the nucleation and growth of Pt induced faceting of W(111).

The main advantage of low energy electron microscopy (LEEM) is that real-time observation of such structural–morphological changes is possible, with ~70 Å spatial resolution under ideal conditions. The low energy electrons that are used to image the surface are diffracted, essentially forming a LEED pattern inside the imaging column of the low energy electron microscope. One has a choice between imaging the LEED pattern and forming a real image of the surface using any of the LEED beams. For a surface that has multiple domains of different surface structures, it is possible to distinguish one domain type from the others when imaging the surface by using a selected LEED spot from that domain structure to form a real space image of the surface. Two of the many excellent examples of this technique are the alternating 2×1 and 1×2 reconstructions on neighboring steps of Si(100) [6–12], and the oxygen induced reconstruction of W(100) with 5×1 and 1×5 domains [13].

The LEED pattern from a faceted bcc(111) surface is a superposition of three distinct bcc(211) patterns. It is possible, therefore, to image the surface through a selected LEED spot belonging to only one of the three facet orientations, and observe individual facets on the surface, provided that the facet size exceeds the resolution limit of the LEEM. Furthermore, under certain conditions a coexistence of faceted and planar regions has been observed using LEED and STM for the Pt/W(111) [14–16], Pd/Mo(111) and Au/Mo (111) systems [4]. With LEEM it is possible to observe the spatial distribution of such coexistence phases. Last, but not least, LEEM is capable of providing a real-time view of the transitions from planar to faceted systems, or planar to coexistence to faceted systems, and vice versa. We observe in these experiments the nucleation and growth of faceted domains as the heated surface is dosed with Pt.

2. Experiment

The experiments were performed at Sandia National Laboratories using a commercial LEEM developed by E. Bauer [5]. The LEEM apparatus is housed in a conventional stainless steel ultrahigh vacuum (UHV) system with an average base pressure of 2×10^{-10} Torr. The chamber is equipped with a Pt evaporation source for dosing the W(111) sample in situ, allowing the observation of the surface while it is being dosed. The sample may also be heated in situ by electron bombardment from the back side. Also available are a K source and an external Hg arc lamp to perform photoemission electron microscopy, necessary for the proper alignment of the microscope and the sample. A quadrupole mass spectrometer may be used for residual gas analysis.

LEEM images and LEED patterns are formed on a channel plate intensifier, and imaged by a phosphor screen. The images are recorded onto video cassettes using a CCD camera. A video image-grabbing software also enables the storage of LEEM pictures on a computer for further analysis.

Attached to the main LEEM chamber are two separate preparation chambers: one for sample cleaning, and the other equipped with a cylindrical mirror analyzer and a concentric electron gun for Auger electron spectroscopy (AES). We use AES to check sample cleanliness and to determine the approximate Pt coverage, using the calibration of Pt to W Auger peak ratio versus coverage of previous works [15,17].

The sample is a W single crystal disk (approx. 1 mm thick and 1 cm in diameter) oriented and mirror-polished to within 0.5° of the (111) plane. A molybdenum sample holder assembly provides for high temperature anneals (up to 2400 K), by using a W filament mounted directly behind the sample for electron bombardment heating, where the sample is kept at a high positive potential (up to 800 V) and is heated by electrons emitted as the filament is heated resistively to incandescence;

at maximum temperatures the emission current reaches 150 mA. The sample is cleaned by flashing above 2400 K in an auxiliary chamber, while lower temperature anneals (up to 1500 K) are performed in the LEEM chamber in situ. The sample temperature is measured using both an infrared pyrometer and a matched filament pyrometer.

Ultrathin Pt films are deposited from a commercial metal evaporator, in which a Mo rod holding a small Pt ball is heated by electron bombardment. The dosing rate is automatically kept constant by monitoring the beam flux. We estimate the maximum accumulation rate at the surface to be approximately 1×10^{14} atoms cm^{-2} min^{-1}, based on AES and LEED observations, as compared with previous experiments in systems equipped with quartz crystal microbalances (QCM). This dosing rate would result in a W(111) surface fully covered by Pt in approximately 15 min. However, the sample is partially covered by a Mo cap as part of the sample holder assembly, in order to achieve more uniform electric fields above the surface. This arrangement, combined with the fact the Pt doser is mounted at an angle of $\sim80°$ off the sample surface normal, results in a significant reduction of the dosed surface area. We estimate that only a ~15–20% central area of the total sample surface is dosed directly. The significance of this arrangement is discussed below.

3. Results and discussion

Previous work has shown that Pt induces faceting of the W(111) surface under certain conditions [15]. A phase diagram has been mapped out (Fig. 1) as a function of Pt coverage and annealing temperature, based on LEED observations. Note that the phase diagram has been updated and the coverage scale rescaled from that in Ref. [15] based on recent temperature programmed desorption experiments as well as measurements using a QCM deposition monitor [17]. A LEED pattern characteristic of a fully faceted surface is observed if the Pt coverage exceeds a critical coverage of one physical monolayer (i.e. every W surface atom is covered by a Pt atom, $\sim1.7\times10^{15}$ atoms cm^{-2}) and the sample is annealed between 750 and 1200 K for 3 min. At coverages between 0.7 and 1 physical monolayer, or if the annealing temperature is between 1200 and 1300 K, LEED shows a combination of a faceted pattern and a planar W(111) pattern. STM experiments have confirmed the coexistence of a planar region with faceted structures [15,16]. It has also been shown using STM that the final facet size increases with increasing annealing temperature, from an average size of ~150 Å at 880 K up to an average size of ~700 Å at 1400 K [14–16].

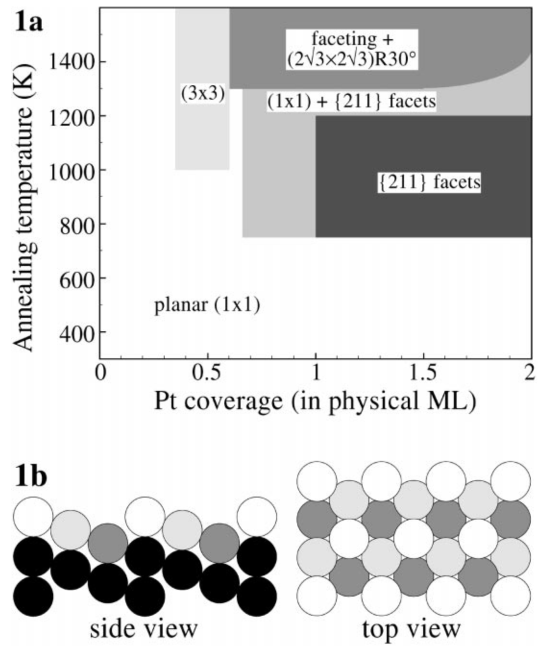

Fig. 1. (a) Phase diagram to demonstrate the temperature and coverage dependence for faceting of W(111) caused by thin Pt films, based on LEED observations. Adapted from Ref. [15], with coverage scale adjusted according to more recent experiments [17]. (b) Top and side view of the W(111) surface demonstrates that atoms from the three outermost layers are exposed to the surface – these three atomic layers together form one physical monolayer.

In view of these earlier results, we have attempted three different sets of experiments to examine the nucleation and growth of faceted regions. First we produced fully or partially faceted surfaces with large facet sizes, expecting to see individual facets that exceed in size the resolution limit of our microscope (which we estimate to be ~200 Å for the conditions in this experiment).

Second, we have dosed Pt in situ onto a hot (~1050 K) surface while observing the system with LEEM, therefore attempting to see a real-time horizontal (i.e. constant temperature) cross-section of our phase diagram: a transition from planar to faceted surface. Finally, we dosed onto a cold surface an amount of Pt sufficient to induce faceting, and gradually increased the surface temperature beyond the faceting threshold, which gives a real-time vertical (i.e. constant coverage) cross-section of the phase diagram. Each of these experiments is discussed below.

3.1. LEED observations

We have used the LEED capability of the microscope to observe faceting and to establish proper dosage levels and annealing temperatures. Since a direct measurement of Pt coverage is not possible to carry out in the LEEM system, we have relied on results of previous work [15], in particular on the phase diagram of Fig. 1. As mentioned earlier, because of an Mo cap covering the sample, only 15–20% of the surface is dosed with Pt. Since the overlayer film diffuses to cover the entire surface under the Mo cap upon high temperature annealing, we have to evaporate several (5–7) physical monolayers of Pt onto this small central area to maintain a fully covered surface at elevated temperature, for faceting to be observable.

The identification of faceting of a W(111) surface using conventional LEED has been well described before [18]. The three-sided pyramids of the faceted W(111) surface have equivalent {211} faces: (211), (121) and (112). Therefore, the LEED pattern of the faceted W(111) surface is a superposition of three distinct W{211} LEED patterns, each rotated 39° *off* the surface normal, and rotated 120° with respect to each other *about* the surface normal. While LEED beams of the W(111) surface converge onto the specular (0,0) beam normal to the surface as the electron energy is increased, LEED spots from the {211} facets will converge onto their respective specular beams, 39° off the surface normal, near the edge of the LEED screen. By varying the energy of the incident electrons and observing the movement of LEED beams, both fully and partially faceted systems are easily identified.

When using the LEED capability of a LEEM, however, the pattern is slightly different (Fig. 2). LEED beams from the planar W(111) surface do not move as the electron energy is changed [19,20], whereas spots from the {211} facets do. In particular, three (0,1) spots from the three different {211} orientations (identified on Fig. 2) move symmetrically across the screen as the incident energy is varied; at ~8 eV incident energy they coincide in the center of the pattern. If the pattern is of a partially faceted surface, they also coincide with the (0,0) beam of the planar surface (cf. Fig. 3); the importance of this fact in identifying facets on real space LEEM images is discussed in Section 3.2.

Our LEED results are in agreement with previous work [15], although the coverage scale of the phase diagram of Fig. 1 has been rescaled based on more recent experiments [17]. The clean surface produces a well-defined 1 × 1 LEED pattern, and using various Pt coverages and annealing temperatures several examples of both partially and fully faceted surfaces have been produced. In addition, the high temperature region on Fig. 1, identified

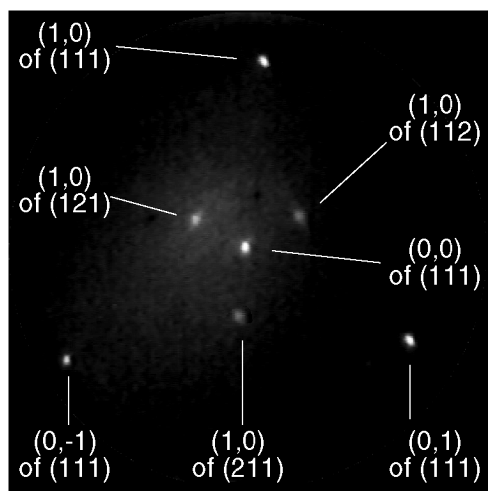

Fig. 2. LEED image of partially faceted W(111) using LEEM at 17 eV incident electron energy. Beams from the planar (111) surface are identified as well as beams from the three different facet orientations: (211), (121) and (112).

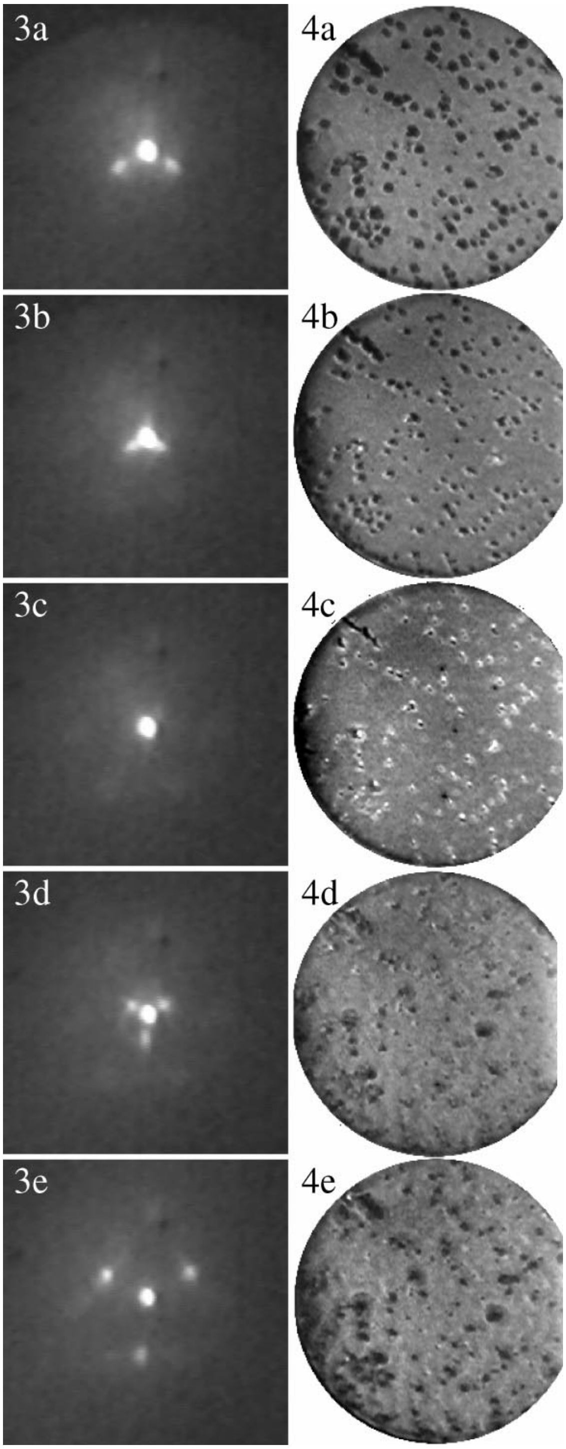

as 'superstructure', has been determined to be $(2\sqrt{3}\times 2\sqrt{3})R30°$.

Of particular interest is the experiment where the initially clean sample is kept at ~1050 K, and observed with LEED while being dosed with Pt. After 60 min of deposition extra beams from {211} facets appear on top of the planar 1×1 pattern, indicating a coexistence of planar W(111) features with {211} facets. Upon further Pt dosing (after 90 min) beams from the planar 1×1 pattern disappear, leaving a fully faceted LEED pattern behind. This is in good qualitative agreement with a 'horizontal' (i.e. constant temperature) cross-section of the phase diagram on Fig. 1. The quantitative agreement between 60 versus 90 min and 0.7 versus 1 physical monolayers is also satisfactory, considering the error involved in exact coverage determinations. The LEEM study of this constant temperature cross-section is discussed below, in Section 3.3.

3.2. General LEEM observations

There are two different methods that can be used to generate LEEM images of a partially faceted surface. One may select – using a small aperture – a LEED beam from the planar surface, such as the (0,0) beam, to form an image of the surface. This is referred to as a 'bright field image', since the planar surface appears bright on the screen, while facets or faceted regions (as well as contaminated areas that do not have the structure of the planar W(111) surface) appear dark (Fig. 4a).

The bright field mode has the advantage that the incident electron energy may be varied at will, since LEED spots from the planar surface remain stationary, and therefore do not leave the imaging aperture. This fact may be used to prove whether the features observed with LEEM are indeed due

Figs. 3 and 4. LEED and bright field LEEM image sequence for a partially faceted surface, with varying incident electron energy: 5.5, 6.5, 8, 9 and 12 eV for images (a)–(e), respectively. The coincidence of the {211} facet LEED beams with the (0,0) beam of the planar surface at ~8 eV corresponds to the brightening of faceted regions on LEEM. (Field of view is ~9 μm. Uncertainty is 5–10% in all field of view data.)

to facets or faceted regions, using the observation that faceted spots coincide with the planar (0,0) beam at an incident energy of 8 eV. Fig. 3 shows a series of LEED patterns from the partially faceted surface at incident energies from 5.5 to 12 eV, and clearly demonstrates the merging of the facet beams with the (0,0) beam of the planar surface at ~8 eV. Fig. 4 shows a series of bright field images at incident energies from 5.5 eV (Fig. 4a) to 12 eV (Fig. 4e). Some of the dark spots visible on Fig. 4a 'light up', as the energy is increased from 5.5 to 8 eV in Fig. 4c, then become dark again as the energy is further increased to 12 eV (Fig. 4e); these initially dark areas therefore are positively identified as being due to faceted regions. The spots that remain dark at 8 eV are probably due to surface contamination or defects.

Previous STM experiments performed on the Pt/W(111) system indicate that the average facet size is expected to be approximately 700 Å for this temperature (1500 K), with fairly narrow size distribution [14–16]. We believe, therefore, that the dark areas, approximately 2000–3000 Å in diameter, do not correspond to individual facets, but rather to small, fully faceted regions of the surface.

Note that faceted regions appear as bright spots when facet LEED beams coincide with the planar (0,0) beam, rather than the entire screen having a uniform brightness. This might be due to differences in the summed LEED beam intensity from the faceted region, in comparison with that from the planar region, or it might be due to focusing effects. Furthermore, the bright spots also appear to have a ring-like structure, with dark dots in the center. We believe that this effect is simply due to the focusing conditions, rather than to contamination at the center of each faceted region.

The second method of forming LEEM images is by selecting one of the LEED beams originating from one of the three {211} facets – this is referred to as a 'dark field image'. Fig. 5a is a dark field image of the *fully* faceted surface approximately 9 μm (9×10^4 Å) across. The sample was prepared by annealing a sample dosed with over 1 physical ML of Pt to ~1200 K (the image was taken at room temperature). According to STM experiments [14,16], facet sizes at this temperature range from 200 to 700 Å. In this case only one side of each pyramid appears bright, while the dark areas include facets of the other two {211} orientations, as well as facets that are smaller than the 200 Å resolution limit. The latter explains why less than one third (~15%) of the total surface area is bright, although according to LEED there are no planar regions (these would also appear dark) on this surface.

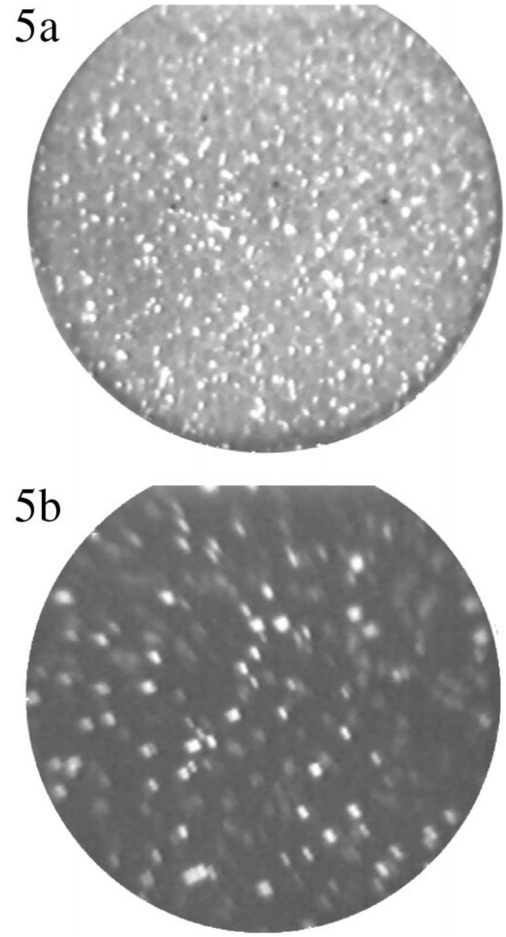

Fig. 5. Dark field image of fully faceted surface [(a) field of view, ~9 μm; electron energy, 12 eV] and partially faceted surface [(b) field of view, ~5 μm; electron energy, 4.6 eV)]. Bright spots are believed to correspond to individual facets.

Fig. 5b is a dark field image of a *partially* faceted surface approximately 5 μm (5×10^4 Å) across. The same surface as above has been annealed to 1400 K (this image was also taken at room temperature). LEED shows a coexistence of planar and faceted patterns, and previous STM experiments show individual pyramids as large as ~1500 Å with extended planar regions [14,16]. The few bright spots on Fig. 5b with rectangular symmetry are probably due to such large facets, comparable to facets in atomic resolution STM images of the faceted Pd/W(111) system [3].

One might argue that small facets are not visible in LEEM because they are smaller than the transfer width of the low energy electron beam. Note, however, that a fully faceted surface with individual facet sizes that prove to be much too small to be observable by LEEM produces a perfectly well-defined LEED pattern. This indicates that the facet size exceeds the transfer width of the electron beam, and the limiting constraint in imaging small facets is the lateral resolution of the microscope. Indeed, fully faceted surfaces for which the maximum facet size is below ~200 Å will appear uniformly gray.

3.3. Real-time LEEM – faceting at constant temperature

The most important advantage of LEEM is its capability for imaging a surface in real time, even surfaces at high temperatures, or surfaces as they are being dosed. The main objective of this project was to conduct real-time observations of the nucleation and growth of Pt induced faceting of W(111).

One set of experiments was aimed at observing the onset of faceting along a horizontal cross-section of the phase diagram of Fig. 1: that is, observing the surface that is kept at a constant temperature as Pt is accumulated at a slow rate, ~1 physical monolayer per 15 min at the center of the sample. Fig. 6 shows a sequence of bright field images from one such experiment, where the sample temperature was kept at 1050 K. After ~60 min well-defined dark spots (indicating small islands of faceted regions) are clearly observable (Fig. 6a). After ~90 min the surface appears uniformly dark, i.e. fully faceted (Fig. 6f).

The time delay of ~60 min until the first signs of faceting (rather than ~10–15 min expected from the dosing rate) is because at 1050 K the Pt readily diffuses over the W(111) surface; Pt may even diffuse to areas under the Mo cap that are not being dosed directly with Pt. Note that desorption of Pt from the W(111) surface does not occur below ~1600 K [15]. The spreading of the Pt film and faceting are two competing processes, until enough Pt is dosed to completely cover the sample everywhere with a film at least a one physical monolayer thick. In fact, if we continue the experiment above, keeping the sample at the same temperature (1050 K) after the surface is fully faceted, but stop the deposition of Pt, the surface reverts to a completely planar form in ~15 min owing to the spreading of the Pt film so that the critical thickness requirement for faceting is no longer met. If at this point we open the Pt doser while keeping the same sample temperature, the surface becomes completely faceted again in less than ~30 min.

The most remarkable result of the above experiment is that the fully faceted surface is achieved through a nucleation and subsequent growth of a relatively few faceted regions. Based on this observation we suggest that the Pt film itself grows via this nucleation/growth process. Note that the critical film thickness for complete faceting is one physical monolayer ($\sim 1.7 \times 10^{15}$ atoms cm^{-2}), which corresponds to covering all exposed W atoms in the top three atom layers, and which is equivalent to three geometrical monolayers using the conventional definition. Just before the first signs of faceting become visible, the surface appears to be covered with ~2/3 physical monolayers (2 geometrical monolayers) of Pt. As the third geometrical monolayer nucleates, and thus the film thickness reaches critical coverage, faceting occurs. The numbers (2/3 versus 1 physical monolayer, 60 min versus 90 min of dosing) are certainly in good agreement with the phase diagram of Fig. 1.

The processes of film growth during deposition of atoms on surfaces, including the nucleation, growth and coalescence of adsorbate islands, are among the best studied phenomena in surface science. Experimental methods range from diffraction techniques (such as SPA-LEED [21] and thermal energy helium-atom scattering [21–23]) to real space observations using STM [24–29], transmission electron microscopy (TEM) and LEEM [30]; theoretical predictions and models also abound [31–36].

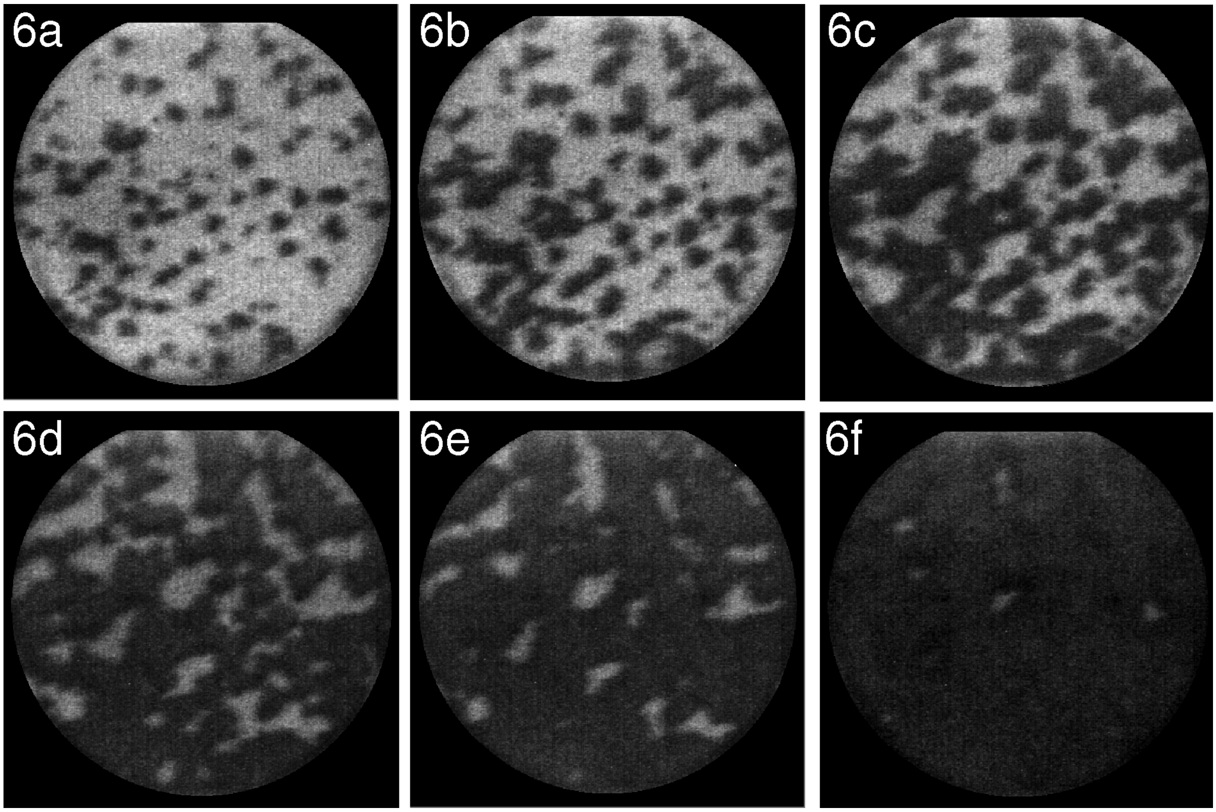

Fig. 6. Bright filed image of nucleation and growth of faceted regions on Pt/W(111) at constant temperature (~1050 K) and constant Pt flux. The dosing times are 63, 69, 75, 81, 87 and 93 min for images (a)–(f), respectively. Field of view is ~5 μm, and incident electron energy is 5.5 eV.

Metal adsorbates, when deposited onto metal surfaces at temperatures ≥300 K, often have high mobility and condense into islands [26,27]. These islands are nucleated either at terrace edges or other surface defects such as screw dislocations (heterogeneous nucleation) [26,30], or simply in the middle of wide terraces, if the adsorbate density is high enough for the spontaneous creation of nuclei where the number of atoms exceeds a critical value (homogenous nucleation) [27,29], or both [24,28].

In our experiments of Pt on W(111), we believe the growth proceeds in a layer-by-layer fashion up to the completion of the first physical monolayer. However, as mentioned above, one physical monolayer includes three geometrical monolayers, where each geometrical monolayer includes adsorbate atoms of the same type of nearest-neighbor environment. Our observations indicate that as Pt is being deposited onto the substrate, the first two geometrical monolayers are completed first; then follows the completion of the third geometrical monolayer via nucleation and subsequent growth of islands. This suggests that while Pt adatoms in the first two monolayers remain relatively stable on the W(111) surface, the Pt atoms deposited on top of this surface have higher mobility, and readily diffuse around until sticking onto an already growing island.

It is important to note that as the faceted regions are growing, there are no new regions being nucleated on the remaining planar surface (Fig. 6). This may be explained by the rapid diffusion of Pt atoms at the elevated temperature of 1050 K, and the very low impingement flux. The combination of the two results in a low probability of additional island nucleation as compared to the growth rate of existing islands. In addition, Pt adatoms diffusing on the surface may stick preferentially to already faceted regions.

Note that the complicated interplay between the faceting process and the diffusion of Pt away from the central region is the reason why the idea of a detailed quantitative analysis or a theoretical model has not been attempted for the present data. To obtain data for such analysis, a better control of experimental conditions is necessary, including an improved sample holder design.

3.4. Real time LEEM – faceting at constant coverage

Another interesting question is, how does faceting occur when the surface is fully covered with Pt beyond the critical coverage, and the sample is heated slowly above the critical temperature of $\sim$750 K? Does the whole surface facet at once, or is there a nucleation and growth type process, much like the above case?

Repeated attempts to observe any type of nucleation and growth process using LEEM for such 'constant coverage' faceting were not successful, even though LEED indicated a fully faceted surface.

The apparent lack of a nucleation and growth type of process (or any other kind of coexistence phase) in a constant coverage faceting experiment is in agreement with previous results. The phase diagram of Fig. 1 from earlier work [15] does not show a coexistence phase at the low temperature boundary of the faceted region – although in those experiments temporal evolution studies were not attempted; the sample was annealed at each temperature for 3 min. Also, detailed STM studies of the initial stages of faceting at constant coverages were conducted for the Pd/W(111) system [37], and the surface was found to undergo a uniform roughening/microfaceting, with facet sizes as small as $\sim$20 Å.

4. Conclusions

We have demonstrated that LEEM is an extremely useful complement to other microscopic and diffraction techniques used to characterize metal film induced faceting of atomically rough bcc(111) surfaces. During Pt deposition onto a heated W(111) substrate we have observed real-time LEEM images of the faceting process, which demonstrate that facets nucleate and grow in spatially separate regions of the surface. The faceted regions grow to cover the entire surface when the Pt coverage reaches $\sim$1 physical monolayer. LEEM also provides a very convenient and immediate comparison of real space images and LEED observations, a particularly useful feature when studying faceting.

5. Outlook

The resolution of LEEM does not match that of STM; however, its convenience and the advantages mentioned above make it very desirable both for identifying new candidates for faceting and for studying the dynamic details of such large scale morphological transformations. In any case, improved sample holder and evaporator designs are both needed for a more thorough and more complete study of the faceting process.

Future LEEM studies of the adsorbate-induced faceting of atomically rough metal surfaces will involve other overlayer metals and possibly other atomically rough substrates (such as an fcc(210) metal surface). Furthermore, there have been literature reports of reversible phase transitions in the case of Pd/Mo(111), Au/W(111) and O/Mo(111) [4,14], where the surface changes from a fully faceted to a coexisting planar/faceted surface structure as the temperature increases and reverts to fully faceted as the temperature decreases. Such phenomena clearly call for a detailed LEEM investigation.

Acknowledgements

This work has been supported, in part, by the US Department of Energy, Office of Basic Energy Sciences. This work was performed at Sandia National Laboratories, Albuquerque, NM. Sandia is a multiprogram laboratory operated by Sandia

Corporation, a Lockheed Martin Company, for the United States Department of Energy under Contract No. DE-AC04-94AL8500.

References

[1] J. Guan, R.A. Campbell, T.E. Madey, Surf. Sci. 341 (1995) 311.
[2] T.E. Madey, J. Guan, C.H. Nien, C.Z. Dong, H.-S. Tao, R.A. Campbell, Surf. Rev. Lett. 3 (1996) 1315.
[3] C.H. Nien, T.E. Madey, Surf. Sci. 380 (1997) L527.
[4] K.-J. Song, J.-C. Lin, M.-Y. Lai, Y.-L. Wang, Surf. Sci. 327 (1995) 17.
[5] E. Bauer, Rep. Prog. Phys. 57 (1994) 895.
[6] M. Mundschau, E. Bauer, W. Telieps, W. Swiech, Surf. Sci. 223 (1989) 413.
[7] E. Bauer, M. Mundschau, W. Swiech, W. Telieps, J. Vac. Sci. Technol. A 9 (1991) 1007.
[8] W. Swiech, E. Bauer, Surf. Sci. 255 (1991) 219.
[9] N.C. Bartelt, R.M. Tromp, E.D. Williams, Phys. Rev. Lett. 73 (1994) 1656.
[10] N.C. Bartelt, R.M. Tromp, Phys. Rev. B 54 (1996) 11 731.
[11] R.M. Tromp, M.C. Reuter, Phys. Rev. Lett. 68 (1992) 820.
[12] J.B. Hannon, N.C. Bartelt, B.S. Swartzentruber, J.C. Hamilton, G.L. Kellogg, Phys. Rev. Lett. 79 (1997) 4226.
[13] M.S. Altman, E. Bauer, Surf. Sci. 347 (1996) 265.
[14] K.J. Song, C.Z. Dong, T.E. Madey, in: S.Y. Tong, M.A.V. Hove, K. Takayanagi, X.D. Xie (Eds.), The Structure of Surfaces III, Springer, Berlin, 1991, p. 378.
[15] C.-Z. Dong, S.M. Shivaprasad, K.-J. Song, T.E. Madey, J. Chem. Phys. 99 (1993) 9172.
[16] T.E. Madey, K.-J. Song, C.-Z. Dong, R.A. Demmin, Surf. Sci. 247 (1991) 175.
[17] K. Pelhos, Ph.D. thesis (1999), Rutgers University.
[18] K.-J. Song, R.A. Demmin, C. Dong, E. Garfunkel, T.E. Madey, Surf. Sci. 227 (1990) L79.
[19] E. Bauer, Ultramicroscopy 17 (1985) 51.
[20] E. Bauer, W. Telieps, Scanning Microscopy, Suppl. I (1987) 99.
[21] P. Bedrossian, B. Poelsema, G. Rosenfeld, L.C. Jorritsma, N.N. Lipkin, G. Comsa, Surf. Sci. 334 (1995) 1.
[22] C. Tölkes, P. Zeppenfeld, M.A. Krzyzowski, R. David, G. Comsa, Phys. Rev. B 55 (1997) 13 932.
[23] G. Vidali, Surf. Rev. Lett. 4 (1997) 709.
[24] S. Horch, P. Zeppenfeld, G. Comsa, Surf. Sci. 331–333 (1995) 908.
[25] P.S. Weiss, D.M. Eigler, Phys. Rev. Lett. 69 (1992) 2240.
[26] D.D. Chambliss, K.E. Johnson, R.J. Wilson, S. Chiang, J. Magn. Magn. Mater. 121 (1993) 1.
[27] R.Q. Hwang, J. Schröder, C. Günther, R.J. Behm, Phys. Rev. Lett. 67 (1991) 3279.
[28] S. Horch, P. Zeppenfeld, G. Comsa, Appl. Phys. A 60 (1995) 147.
[29] J.A. Meyer, P. Schmid, R.J. Behm, Phys. Rev. Lett. 74 (1995) 3864.
[30] M. Mundschau, E. Bauer, W. Telieps, W. Swiech, Surf. Sci. 213 (1989) 381.
[31] M. Zinke-Allmang, L.C. Feldman, M.H. Grabov, Surf. Sci. Rep. 16 (1992) 377.
[32] J.B. Hannon, M.C. Bartelt, N.C. Bartelt, G.L. Kellogg, Surf. Rev. Lett. 5 (1998) 1159.
[33] M. Breeman, T. Michely, G. Comsa, Surf. Sci. Lett. 370 (1997) L193.
[34] Y. Li, A.E. De Pristo, Surf. Sci. 351 (1996) 189.
[35] M.C. Bartelt, J.W. Evans, Surf. Sci. 298 (1993) 421.
[36] V.P. Zhdanov, Surf. Sci. 392 (1997) 185.
[37] C.-H. Nien, Ph.D. Thesis, Rutgers University.